Molecular Fingerprints in the Electronic Properties of Crystalline Organic Semiconductors: From Experiment to Theory

S. Ciuchi,[1] R. C. Hatch,[2] H. Höchst,[3] C. Faber,[4] X. Blase,[4] and S. Fratini[4]

[1]*Istituto dei Sistemi Complessi CNR, CNISM and Dipartimento di Fisica, Università dell'Aquila, via Vetoio, I-67100 Coppito-L'Aquila, Italy*

[2]*Department of Physics and Astronomy, Aarhus University, 8000 Aarhus C, Denmark*

[3]*Synchrotron Radiation Center, University of Wisconsin-Madison, 3731 Schneider Drive, Stoughton, Wisconsin 53589, USA*

[4]*Institut Néel-CNRS and Université Joseph Fourier, Boîte Postale 166, F-38042 Grenoble Cedex 9, France*

(Received 10 January 2012; revised manuscript received 19 April 2012; published 18 June 2012)

By comparing photoemission spectroscopy with a nonperturbative dynamical mean field theory extension to many-body *ab initio* calculations, we show in the prominent case of pentacene crystals that an excellent agreement with experiment for the bandwidth, dispersion, and lifetime of the hole carrier bands can be achieved in organic semiconductors, provided that one properly accounts for the coupling to molecular vibrational modes and the presence of disorder. Our findings rationalize the growing experimental evidence that even the best band structure theories based on a many-body treatment of electronic interactions cannot reproduce the experimental photoemission data in this important class of materials.

DOI: 10.1103/PhysRevLett.108.256401 PACS numbers: 71.38.−k, 71.20.Rv, 73.50.Gr, 79.60.Fr

Introduction.—Organic semiconductors are key materials for future applications ranging from flexible electronics to photovoltaics [1]. Because of the weakness of van der Waals intermolecular bonds, these materials are commonly believed to stand in an intricate region between the molecular limit and the extended band picture, calling for concepts that go beyond the standard paradigms of inorganic semiconductors. Experimental charge transport and optical studies over the past few years have indeed given contrasting indications on the nature of the electronic carriers. The existence of low-mass quasiparticles indirectly inferred from optical sum rules [2], and the apparently "bandlike" temperature dependent electronic mobilities observed in the best crystalline systems [3–6] are difficult to reconcile—within the framework of band theory alone—with absolute values of the mobility that hardly exceed few tens of $\mathrm{cm}^2/\mathrm{Vs}$. The coupling to molecular vibrations as well as the presence of disorder are often regarded as the primary causes of the poor conductive properties of this broad class of materials [7], as both phenomena can slow down the electron motion in the already narrow bands constructed from π-intermolecular overlaps. Still, no direct proof on how such microscopic mechanisms affect the electronic states has been given to date.

As of today, while the strongest efforts are devoted to understanding and improving their charge transport characteristics, a proper description of even the most basic electronic properties such as the band dispersion and carrier lifetime—the foundations of our understanding of conventional semiconductors—remains a challenge in organic semiconductors. Recent angle resolved photoemission (ARPES) experiments performed on crystalline samples [8–13] have evidenced that the best band structure theories based on a many-body treatment of electronic interactions cannot reproduce the experimental spectra, as they predict electronic bandwidths that are significantly smaller than those measured experimentally. Here we provide a combined theoretical and experimental analysis of the ARPES spectra of pentacene—a material that is often regarded as a model compound for organic molecular solids. By focusing on the full momentum dependence of the spectral features, we demonstrate that the interaction of electrons with the internal vibrations of the molecules deeply modifies the nature of the extended electronic states. The multiple vibrational overtones that are commonly observed in angle-integrated photoemission spectra [14–16] translate into a complex fine-structure in momentum space, unveiling an unexpectedly large separation of the electronic bands that is ultimately responsible for the observed increase of the total bandwidth. Analogous molecular fingerprints are predicted to affect the electronic bands of broad classes of molecular systems including organic semiconductors, charge-transfer organic salts, and doped organic conductors [17].

Photoemission experiment.—In order to probe the effect of electron-molecular vibration interactions on the electronic spectra of organic solids, ARPES experiments were performed on *in situ* grown pentacene films of thickness $d >$ 100 Å deposited on Bi(001). This is in contrast with previous experiments performed on organic monolayers [8,15,16], where the energy-momentum dispersion could be seriously affected by the binding to the substrate. All experiments were carried out at the University of Wisconsin Synchrotron Radiation Center (SRC). A detailed description of the sample preparation process and of the resulting crystalline film including lattice constants **a** and **b** are reported elsewhere [10,18]. The combined photon and electron energy resolution was $\Delta E \sim 40$ meV, and for 15 eV photons (used in most

experiments) the electron momentum resolution was $\Delta k_{\|} < 0.03$ Å^{-1}. Figure 1(a) shows the photoemission spectra measured at $T = 75$ K near the top of the highest occupied molecular orbital (HOMO) as a function of parallel momentum $k_{\|}$ along the path illustrated in the inset of Fig. 1(c). Since the lattice structure has two molecules per unit cell, two dispersive branches can be identified, that we denote as $H1$ and $H2$. The dots in Fig. 1(a) are the positions of the two most prominent peaks at each given $k_{\|}$, as obtained from Gaussian fits to the individual spectra. The solid lines are the band dispersions obtained from state-of-the-art *ab initio* calculations for the crystalline film phase which corresponds to the pentacene polymorph of our sample [19,20]. It is apparent that the separation between the $H1$ and $H2$ branches in the experiment is much larger than predicted. As a consequence the measured total HOMO bandwidth, $W_{\text{exp}} = 450 \pm 15$ meV, defined as the distance between the $H1$ and $H2$ peaks at the $\bar{M}$ point (see Supplemental Material [18]), is also much larger than the calculated values for the pentacene crystalline film phase, both within density functional theory (DFT) [19] ($W_0 = 348$ meV), and within the more accurate GW method [21] ($W_0 = 360$ meV). The discrepancy is well beyond the experimental uncertainty, which confirms the systematic findings reported in the most recent ARPES measurements on pentacene and rubrene [8–13]. This indicates that the band structure calculations alone—even including electronic many-body correlations as is done in Ref. [21]—are not sufficient to properly describe the observed excitation spectra.

Theoretical modeling.—In order to solve the discrepancy between theory and experiment, we now calculate the photoemission spectral function by considering the coupling of holes in the HOMO band with the high-frequency, intramolecular vibrations arising from the carbon-carbon stretching forces. We use a nonperturbative, theoretical method in order to avoid any *a priori* assumption on the relative importance of the different phenomena at work. This is a crucial issue since in organic semiconductors the characteristic energy scales, namely (a) the electronic bandwidth W_0, proportional to the intermolecular electronic transfer energies, (b) the strength of the electron-molecular vibration (EMV) coupling, measured by the structural relaxation energy E_P associated with adding a charge to a molecule, (c) the molecular vibrational energies, and (d) the energy fluctuations due to disorder, that cannot be ignored when dealing with real systems, are all of comparable magnitude (~ 0.1 eV). This means that no small parameter can be identified that would allow application of perturbation theory. The microscopic parameters of the EMV interaction specific to pentacene are obtained here via accurate many-body *ab initio* calculations within the GW formalism [18,22–25]. This method has been shown to yield much better electron-phonon coupling potentials as compared to standard DFT-LDA (local density approximation) calculations in the case of π-conjugated fullerenes [24] and graphene [25]. We then calculate the resulting photoemission spectrum via dynamical mean field theory (DMFT) [26,27], which is able to address in an unbiased way the intricate physical regime of interest in organic semiconductors. The DMFT scheme also allows one to include the presence of disorder that is expected to be relevant in experimental samples, in the form of spatial fluctuations of the molecular energy levels. Experimental estimates of the energy spread Δ range from few tens of meV in single crystals to $\Delta \sim 0.1$ eV or above in amorphous samples [28]. Our crystalline films should be located between these two limits as indicated by the sharpness of our reflection high-energy electron diffraction (RHEED) patterns. Finally, the interaction with low-frequency vibrations of the molecules [14,29], in the range $\hbar\omega \lesssim 40$ meV, is effectively included in the

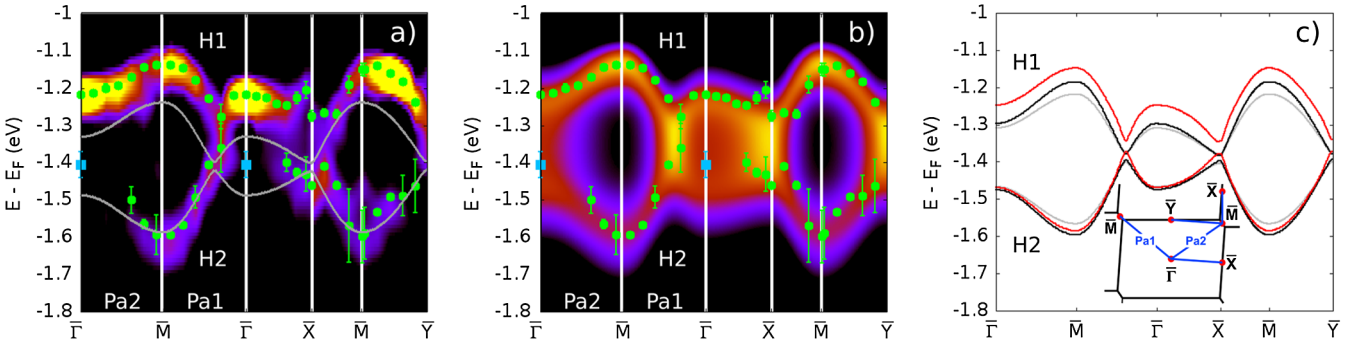

FIG. 1 (color online). (a) Color density plot of experimental ARPES data. The second derivative of the data has been taken to best visualize the energy positions of the dispersive features. The (green) dots are the peak positions as derived from Gaussian fits of the individual spectra. The (blue) square corresponds to a scan with a different incoming photon energy, which recovers the $H2$ spectral weight around $\bar{\Gamma}$ that is hidden due to the matrix element dependence on the photon incoming energy (see the Supplemental Material [18]). The gray line is the *ab initio* band dispersion from Ref. [19]. (b) Calculated spectrum in the presence of EMV interactions and disorder (see text). The dots are the experimental peak positions from panel (a). (c) Theoretical HOMO band dispersion, as obtained from the poles of the spectral function. *Ab initio* (light gray), disordered (black: $\Delta = 75$ meV, $E_P = 0$), and with EMV interactions (dark gray [red]: $\Delta = 75$ meV, $E_P = 69$ meV). The inset shows the corresponding path in the Brillouin zone.

calculation via an increased value of Δ. These low-frequency modes related both to the large molecular size and to the mechanical softness of the material do not give rise to observable features in the photoemission spectra—as their energy lies below the experimental resolution—but they do act as an additional intrinsic source of fluctuation for the molecular energy levels [30,31].

Molecular origin of the band separation.—Fig. 1(b) is a color density plot of the hole spectral function obtained from the theory including both molecular and itinerant aspects on the same footing, as described in the preceding paragraph. We take the calculated value $E_P = 69$ meV for the molecular relaxation energy (corresponding to a reorganization energy $2E_P = 138$ meV), $\hbar\Omega = 174$ meV for the average energy of intramolecular vibrations (see Supplemental Material [18]), a noninteracting bandwidth $W_0 = 348$ meV, and assume a total disorder strength $\Delta = 75$ meV. The similarity with the experimental spectra is remarkable. The most striking point is that the separation between the $H1$ and $H2$ bands is much larger than in the band-structure prediction, restoring the agreement with the locus of the experimental peaks (dots). Also in agreement with the experiment, the features of the calculated spectrum exhibit a considerable broadening, a point that will be discussed below.

To ascertain the microscopic origin of the observed $H1/H2$ separation, Fig. 1(c) shows the HOMO band dispersion obtained from the theory upon the subsequent inclusion of disorder (black curve) and EMV interactions (dark gray [red] curve) on top of the band structure (light gray), as parametrized in Ref. [19]. Disorder in the molecular energy levels causes a rather uniform increase of the band dispersion, but does not modify the overall band shape [32]. Instead, adding the interaction with high-frequency molecular vibrations causes a sizable upward shift of the $H1$ band, leaving the $H2$ band dispersion essentially unchanged from the noninteracting case. This shift is caused by the molecular relaxation energy gain E_P, that is reflected in the extended states of the solid through a stabilization of the $H1$ branch. We conclude that the interplay between EMV coupling and disorder is at the origin of the large $H1/H2$ separation observed in the experiment. The present analysis confirms the results obtained in Ref. [30] based on a related one-dimensional model.

Spectral hallmarks of EMV interactions.—Having shown that the main dispersive features of the ARPES data can be explained by the proper inclusion of interactions with high-frequency molecular vibrations and a moderate amount of disorder, we now proceed to show that additional hallmarks of the EMV coupling are seen in the angle-resolved spectra, providing support to the proposed scenario. Figure 2(a) reports the photoemission intensity measured at the $\bar{M}$ point (full line), and Fig. 2(b) is the corresponding calculated spectrum. In addition to the $H1$ and $H2$ peaks that are clearly resolved, an extra feature can be actually recognized, whose existence is substantiated by

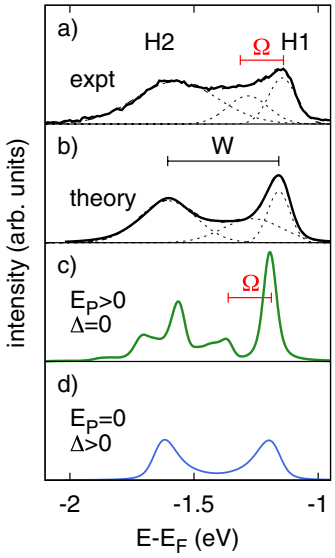

FIG. 2 (color online). (a) Photoemission spectrum measured at the $\bar{M}$ point. The dashed line is a fit of the data with three Gaussian peaks. (b) Calculated spectrum and fit. Parameters are $E_P = 69$ meV and $\Delta = 75$ meV. W is the total bandwidth defined as the distance between the $H1$ and $H2$ peak. (c) The fine structure induced by the EMV interaction is unveiled by removing the disorder in the calculation. (d) The calculated spectrum in the absence of EMV interactions, but with the same degree of disorder. In (b), (c), and (d) the spectrum has been convoluted with a Gaussian of FWHM = 40 meV to mimic the experimental resolution.

fitting the spectra with three Gaussian peaks (dashed lines). Being located at a distance $\simeq \hbar\Omega$ from the main $H1$ peak, it is tempting to associate this feature with a vibrational overtone of the main electronic excitation. That this is indeed the case is demonstrated by repeating the theoretical calculation in the absence of disorder, which reveals all the fine structure that is otherwise smeared out by the energy fluctuations [Fig. 2(c)]. The overtone actually disappears as expected when the EMV interaction is turned off [Fig. 2(d)].

Our analysis shows that the presence of multiple vibrational overtones is also at the origin of the large broadening of the $H2$ peaks observed in the experiment, whose tails extend to very large binding energies [see both Fig. 2(a) and 2(b)]. The reduced lifetime of the $H2$ states again results from a nontrivial interplay between vibrational shakeoff excitations and disorder. The individual resonances contributing to the $H2$ weight are not resolved in the experiment, as these merge into a single broad feature due to the presence of disorder. Such vibrational overtones are however clearly revealed in the calculation on a perfectly ordered crystal [Fig. 2(c)] and could possibly be detected in future experiments on cleaner samples. A more detailed discussion on the interplay between EMV interactions and disorder, not limited to the representative $\bar{M}$ point considered here, is presented in the Supplemental Material [18].

Quantitative analysis and discussion.—Finally we show that combining model Hamiltonian studies with *ab initio* calculations as we have done here can actually be used to extract quantitative information on the relevant microscopic parameters of the materials directly from the experiment. Figure 3(a) illustrates the evolution of the total calculated HOMO bandwidth W resulting from the molecular relaxation phenomenon as a function of the EMV coupling strength $\lambda = 2E_P/W_0$, for different values of the disorder parameter Δ. Taking the calculated value, $E_P = 69$ meV, our experimental data are compatible with a total disorder strength $\Delta = 75 \pm 15$ meV, in agreement with the values available in the literature [28]. As mentioned previously, this is an effective parameter that also includes the intrinsic fluctuations originating from the low-frequency molecular vibrations, whose contribution can be estimated to ≈ 20 meV [29,30]. The estimate $\Delta = 75$ meV given above therefore constitutes an upper bound to the actual structural disorder present in the sample. We note that the value of the molecular relaxation energy itself could be extracted from the experiment if a precise independent estimate of the disorder fluctuations were available.

Beyond these quantitative considerations, the present study clearly establishes the theoretical framework that should be worked with in upcoming studies of transport properties, since a good description of the momentum and energy dependence of carriers is a necessary basis to properly assess mobility properties. In particular, our results show unequivocally that the total HOMO bandwidth *increases* with the EMV coupling. This behavior is opposite to the bandwidth *decrease* that constitutes the basis of most theories of charge transport in organic semiconductors, but that is only expected to apply in the molecular limit, $W_0 \ll \hbar\Omega$ [7,33,34]. Upon closer inspection, we find that a partial band shrinking occurs in a restricted energy range, roughly within a window $\hbar\Omega$ from the top of the band (the ground state for holes) [27]. The width of the $H1$ branch along Pa2, reported in Fig. 3(b), indeed shows a moderate decrease upon increasing the EMV coupling, which however does not obey the textbook [34] exponential renormalization $\propto \exp(-E_P/\hbar\Omega)$ (dashed line). The fact that the phenomenon of band narrowing is shown here to play a reduced role should be taken into account when constructing a theory for charge transport in organic semiconductors.

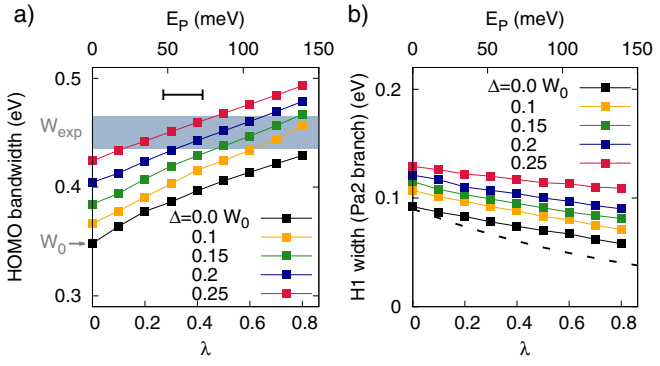

FIG. 3 (color online). (a) Calculated HOMO bandwidth as a function of the EMV coupling strength for different values of the disorder parameter. The shaded area is the measured value (see text). The horizontal bar indicates the range of calculated E_P values in the literature. (b) Renormalization of the $H1$ band along Pa2 ($\bar{M}$-$\bar{\Gamma}$ distance, see Fig. 1). The dashed line is the polaronic renormalization expected in the molecular limit.

Concluding remarks.—There is growing experimental evidence that the electronic properties of organic molecular semiconductors cannot be understood within the commonly accepted band structure picture that prevails for inorganic semiconductors. This discrepancy entails that a consistent description of the extended states in molecular solids should take full account of the microscopic processes taking place at the molecular level. The analysis presented here indeed demonstrates that the proper inclusion of the interaction with molecular vibrations and disorder, beyond electronic band theory calculations, provides a remarkably accurate description of the experimental photoemission spectra in pentacene. The coexistence of dispersive features characteristic of the extended band regime, together with multiphonon shakeoff resonances reminiscent of the molecular spectra, provides solid spectroscopic evidence for the widespread idea that organic materials are located in a crossover region where the band and molecular characters are inextricably linked.

Ab initio calculations have been performed on the supercomputing IDRIS and CIMENT facilities. This work is based in part upon research conducted at the Synchrotron Radiation Center, University of Wisconsin-Madison, which is supported by the National Science Foundation under Award No. DMR-0537588. We acknowledge stimulating discussions with D. L. Huber as well as financial support by the Lundbeck Foundation. We thank A. Morpurgo and G. Profeta for a critical reading of the manuscript.

[1] S. R. Forrest, Nature (London) **428**, 911 (2004).
[2] Z. Q. Li, V. Podzorov, N. Sai, M. C. Martin, M. E. Gershenson, M. Di Ventra, and D. N. Basov, Phys. Rev. Lett. **99**, 016403 (2007).
[3] V. Podzorov, E. Menard, J. A. Rogers, and M. E. Gershenson, Phys. Rev. Lett. **95**, 226601 (2005).
[4] T. Sakanoue and H. Sirringhaus, Nat. Mater. **9**, 736 (2010).
[5] C. Liu, T. Minari, X. Lu, A. Kumatani, K. Takimiya, and K. Tsukagoshi, Adv. Mater. **23**, 523 (2011).
[6] N. A. Minder, S. Ono, Z. Chen, A. Facchetti, and A. F. Morpurgo, Adv. Mater. **24**, 503 (2012).
[7] V. Coropceanu *et al.*, Chem. Rev. **107**, 926 (2007).
[8] H. Kakuta, T. Hirahara, I. Matsuda, T. Nagao, S. Hasegawa, N. Ueno, and K. Sakamoto, Phys. Rev. Lett. **98**, 247601 (2007).
[9] M. Ohtomo, T. Suzuki, T. Shimada, and T. Hasegawa, Appl. Phys. Lett. **95**, 123308 (2009).

[10] R. C. Hatch, D. L. Huber, and H. Höchst, Phys. Rev. B **80**, 081411(R) (2009).
[11] R. C. Hatch, D. L. Huber, and H. Höchst, Phys. Rev. Lett. **104**, 047601 (2010).
[12] S. Machida, Y. Nakayama, S. Duhm, Q. Xin, A. Funakoshi, N. Ogawa, S. Kera, N. Ueno, and H. Ishii, Phys. Rev. Lett. **104**, 156401 (2010).
[13] H. Ding, C. Reese, A. J. Mäkinen, Z. Bao, and Y. Gao, Appl. Phys. Lett. **96**, 222106 (2010).
[14] M. Malagoli, V. Coropceanu, D. A. da Silva Filho, and J. L. Brédas, J. Chem. Phys. **120**, 7490 (2004).
[15] H. Yamane, S. Nagamatsu, H. Fukagawa, S. Kera, R. Friedlein, K. K. Okudaira, and N. Ueno, Phys. Rev. B **72**, 153412 (2005).
[16] S. Kera, H. Yamane, and N. Ueno, Prog. Surf. Sci. **84**, 135 (2009).
[17] W. L. Yang *et al.*, Science **300**, 303 (2003).
[18] See Supplemental Material at http://link.aps.org/supplemental/10.1103/PhysRevLett.108.256401 for more details on sample preparation and ARPES experiments, *ab initio* determination of microscopic parameters, and calculation of the spectral function.
[19] H. Yoshida and N. Sato, Phys. Rev. B **77**, 235205 (2008).
[20] The overall vertical position of the *ab initio* prediction has been adjusted to match the experimental $H2$ band. This is because the dispersion of the $H2$ branch is mostly unaffected by the EMV interaction and should therefore reasonably agree with the band-structure calculation [see Fig. 1(c)].
[21] M. L. Tiago, J. E. Northrup, and S. G. Louie, Phys. Rev. B **67**, 115212 (2003).
[22] F. Aryasetiawan and O. Gunnarsson, Rep. Prog. Phys. **61**, 237 (1998).
[23] X. Blase, C. Attaccalite, and V. Olevano, Phys. Rev. B **83**, 115103 (2011).
[24] C. Faber, J. L. Janssen, M. Cote, E. Runge, and X. Blase, Phys. Rev. B **84**, 155104 (2011).
[25] M. Lazzeri, C. Attaccalite, L. Wirtz, and F. Mauri, Phys. Rev. B **78**, 081406 (2008).
[26] A. Georges, G. Kotliar, W. Krauth, and M. J. Rozenberg, Rev. Mod. Phys. **68**, 13 (1996).
[27] S. Ciuchi, F. de Pasquale, S. Fratini, and D. Feinberg. Phys. Rev. B **56**, 4494 (1997).
[28] W. L. Kalb, S. Haas, C. Krellner, T. Mathis, and B. Batlogg, Phys. Rev. B **81**, 155315 (2010).
[29] A. Girlando, L. Grisanti, M. Masino, A. Brillante, R. G. Della Valle, and E. Venuti, J. Chem. Phys. **135**, 084701 (2011).
[30] S. Ciuchi and S. Fratini, Phys. Rev. Lett. **106**, 166403 (2011).
[31] S. Fratini and S. Ciuchi, Phys. Rev. B **72**, 235107 (2005).
[32] This is a known result for disordered systems that can be formally understood, for example, by solving for the electron propagator in the coherent potential approximation (CPA); see Ref. [31].
[33] T. Holstein, Ann. Phys. **8**, 343 (1959).
[34] G. D. Mahan, *Many-Particle Physics* (Plenum, New York, 1990), 2nd ed..